ISTANBUL TECHNICAL UNIVERSITY ★ GRADUATE SCHOOL

THE EFFECT OF SUCCESSIVE QUENCHING AND AUSTEMPERING HEAT TREATMENTS ON THE MICROSTRUCTURE OF A HIGH SILICON STEEL

M.Sc. THESIS

Şeyma UĞUR

Department of Metallurgical and Materials Engineering

Materials Engineering Programme

NOVEMBER 2024

ISTANBUL TECHNICAL UNIVERSITY ★ GRADUATE SCHOOL

THE EFFECT OF SUCCESSIVE QUENCHING AND AUSTEMPERING HEAT TREATMENTS ON THE MICROSTRUCTURE OF A HIGH SILICON STEEL

M.Sc. THESIS

Şeyma UĞUR
(506201407)

Department of Metallurgical and Materials Engineering

Materials Engineering Programme

Thesis Advisor: Prof. Dr. Murat BAYDOĞAN

NOVEMBER 2024

İSTANBUL TEKNİK ÜNİVERSİTESİ ★ LİSANSÜSTÜ EĞİTİM ENSTİTÜSÜ

ARDIŞIK SU VERME VE ÖSTEMPERLEME ISIL İŞLEMLERİNİN YÜKSEK SİLİSYUMLU BİR ÇELİĞİN MİKROYAPISINA ETKİSİ

YÜKSEK LİSANS TEZİ

Şeyma UĞUR
(506201407)

Metalurji ve Malzeme Mühendisliği Anabilim Dalı

Malzeme Mühendisliği Programı

Tez Danışmanı: Prof. Dr. Murat BAYDOĞAN

KASIM 2024

Şeyma UĞUR, a M.Sc. student of ITU Graduate School student ID 506201407, successfully defended the thesis entitled "THE EFFECT OF SUCCESSIVE QUENCHING AND AUSTEMPERING HEAT TREATMENTS ON THE MICROSTRUCTURE OF A HIGH SILICON STEEL", which she prepared after fulfilling the requirements specified in the associated legislations, before the jury whose signatures are below.

Thesis Advisor :	**Prof. Dr. Murat BAYDOĞAN** İstanbul Technical University	.....
Jury Members :	**Prof. Dr. Hüseyin ÇİMENOĞLU** Istanbul Technical University	.....
	Dr. Hadi JAHANGİRİ Koç University	.....

Date of Submission : 18 October 2024
Date of Defense : 8 November 2024

To my dad,

FOREWORD

I would like to sincerely convey my gratitude and appreciation to my supervisor, Prof. Dr. Murat BAYDOĞAN, for his guidance and supporting me.

I would like to express my sincere thanks to Res. Assist. Erdem BALCI from ITU Metallurgical and Materials Engineering for helping me anytime I need support.

Additionally, I would want to convey to Şencan ÖZKAN, Burak EVREN, Seda YILDIZ and all BAYKAR Materials and Special Process team members for their great supports during my experimental studies.

I would like to state to dedicate my thesis to my precious family. I could not thank my father Ahmet UĞUR enough, who contributed the most to my education, my career, and my entire life. Even though he will not be able to see these now, I will always work to be a person worthy of all his efforts as long as I exist. Additionally I will always be grateful to my mother Melahat UĞUR for unconditional love and support. My deepest appreciation is to my precious sister Kübra UĞUR and my preicious brother Anıl UĞUR for giving me great strength and being behind me every step I take. Additionally I would want to express my profound affection to my cherished nephew İloş for introducing me to the wonders of life and captivating me with her adorable nature. I would like to point out that my gratitude to Hilal UĞUR, who joined our family later but always made me feel like one of the family. I would also like to thank Seyfullah ÖRNEK, a future graduate engineer who is one of my biggest academic supporters and whom I can hold as an example when it comes to engineers with all his skills.

October 2024

Şeyma UĞUR
(Metallurgy and Materials Engineer)

TABLE OF CONTENTS

Page

ABBREVIATIONS

ASTM	**:** American Society of Testing Materials
BF	**:** Bainitic Ferrite
DIT	**:** Direct Isothermal Treatment
M_f	**:** Martensite Finish Temperature
M_s	**:** Martensite Start Temperature
PM	**:** Pre-existing Martensite
QBT	**:** Quench and Bainitic Transformation
TTT	**:** Time – Temperature – Transformation
XRD	**:** X-Ray Diffraction

SYMBOLS

y	**:** Martensite volume fraction
T	**:** Quenching temperature
α	**:** Constant

LIST OF TABLES

Page

LIST OF FIGURES

Page

THE EFFECT OF SUCCESSIVE QUENCHING AND AUSTEMPERING HEAT TREATMENTS ON THE MICROSTRUCTURE OF A HIGH SILICON STEEL

SUMMARY

Quenching and tempering are very common heat treatment methods for low- and high-alloy steels that have sufficient carbon to achieve high strength. Austempering is an isothermal heat treatment utilized to produce bainite with various morphologies in the microstructure in order to obtain good toughness, high wear resistance, and less distortion. However, to obtain maximum benefit from this heat treatment, two important issues should be considered. The first one is the formation of carbides in microstructures, which can be suppressed using high-Si steels. The other is that the bainite transformation may take a very long time to complete, which needs to be accelerated by forming martensite in the microstructure before the bainite transformation. In this point of view, martensitic-bainitic duplex microstructures have the potential to offer a superior strength-toughness combination, as opposed to fully martensitic or fully lower bainitic microstructures. By increasing the nucleation sites at the martensite-austenite interface, the ensuing bainite transition may be sped up and improved mechanical characteristics can be achieved. This study was therefore undertaken to investigate the effect of different quenching temperatures below Ms, which form different volume fractions of martensite, on the bainite morphology developed during the subsequent austempering heat treatment and on hardness as a measure of the mechanical properties of the successively quenched and austempered steel.

Quenching and austempering heat treatments were successively applied to high-Si steel in this study. For the quenching heat treatments, the Ms temperature was first determined to be 250 °C by using JMatPro software. Then the specimens were austenitized at 900 °C for 30 min and quenched in a salt bath at 180, 200, 220, and 240 °C (70, 50, 30, and 10 °C below the Ms temperature, respectively) to form different volume fractions of martensite in the microstructure. The quenched samples were then austempered at 280 °C for 2 hours. After the quenching and austempering heat treatments, it was seen that the microstructure was mainly composed of martensite and bainite. The volume fraction of martensite decreases and the volume fraction of bainite increases, which is accompanied by a decrease in hardness, with the increase in the quenching temperature. X-ray diffraction (XRD) analysis indicated that a small amount of retained austenite exists in the microstructure. Variation of the bainite morphology was also evaluated depending on the quenching temperature. In addition to hardness, tensile, impact and fatigue properties were also examined; The yield and tensile strength of martensitic and bainitic duplex microstructured steels are higher than the microstructure consisting fully of bainite. These values are 1920 MPa, 2050 MPa, 1825 MPa, 1910 MPa, respectively. In terms of impact properties, the microstructure consisting fully of bainite has an impact energy of 33 J, while the impact energy of the martensite and bainitic duplex structure is 10 J. Therefore, it is

determined that as the bainite ratio increases and the martensite ratio decreases in the structure, the impact resistance increases. No significant difference could be detected in fatigue properties, as in other mechanical properties.

ARDIŞIK SU VERME VE ÖSTEMPERLEME ISIL İŞLEMLERİNİN YÜKSEK SİLİSYUMLU BİR ÇELİĞİN MİKROYAPISINA ETKİSİ

ÖZET

Su verme ve temperleme, yüksek dayanım elde etmek için yeterli karbona sahip düşük ve yüksek alaşımlı çelikler için çok yaygın bir ısıl işlem yöntemidir. Östemperleme, iyi tokluk, yüksek aşınma direnci ve daha az distorsiyon elde etmek amacıyla mikroyapıda farklı morfolojilere sahip beynit oluşturmak için uygulanan izotermal bir ısıl işlemdir. Ancak bu ısıl işlemden maksimum faydanın alınabilmesi için iki önemli hususun dikkate alınması gerekmektedir. Bunlardan ilki, yüksek Si içeren çelik kullanarak mikroyapıda karbür oluşumunun engellenmesidir. Diğeri ise beynit dönüşümünün tamamlanmasının çok uzun zaman alabileceği, beynit dönüşümünden önce mikroyapıda martensit oluşturularak bu sürecin hızlandırılması gerektiğidir. Bu açıdan bakıldığında martensitik-beynitik dubleks mikroyapılar, tamamen martensitik veya tamamen alt beynitik ya da tamamen martensitten oluşan mikroyapıların aksine üstün bir dayanım-tokluk kombinasyonu sunma potansiyeline sahiptir.

Beynitik dönüşümden önce yapıda martensit oluşturulmasının mikroyapıdaki etkilerine bakıldığında da martensitin tercihen östenit-östenit (γ-γ) arayüzeyinde veya öncül östenit tane sınırlarında (prior austenite grain boundaries) çekirdeklendiği yaygın olarak kabul edilmektedir. Su vermenin ardından yapılan izotermal bir işlem, dönüşüm tamamlanmadan atermal martensit üretimini durdurur. Bu, çekirdeklenme için olası yerler olarak hizmet edebilecek martensit-östenit (α′-γ) arayüzlerini içeren bir mikroyapının oluşmasını sağlar. İlk oluşan atermal martensitin hacim oranının ve dolayısıyla α'-γ arayüz yoğunluğunun artması, Ms'nin ötesinde izotermal dönüşümü hızlandıracaktır. Pek çok çalışmada yapıda önceden oluşan martensitin kinetik olarak beynitik dönüşümünü hızlandırmasının yanı sıra mekanik özellikleri de geliştirdiği belirtilmiştir.

Mekanik özelliklere etkisi analiz edildiğinde; beynit yapısı iğnesel tanelerden oluşmaktadır ve bu iğnesel tanelerin boyutları değiştikçe tokluk ve dayanım özellikleri değişmektedir. Dolayısıyla optimum dayanım-tokluk kombinasyonu oluşturmak için mikroyapıda beyniti oluşturan iğnesel tanelerin boyutlarının kontrol altına alınması önemli bir araştırma konusu olmuştur. Bu çalışmalarda özellikle iğnesel tanelerin incelmesinin sağlanması ve bu sayede ultra-ince alt beynitik bir mikroyapı oluşturulmasıdır. Oluşturulan bu ultra-ince beynitik yapı ise dayanım özelliklerinin gelişmesine katkı sağlamaktadır. Bu yapının elde edilmesi de birkaç parametrenin değiştirilmesine bağlıdır. Etkili olduğu düşünülen yöntemlerden biri yapıda önceden oluşturulan martensitin beynit iğnesel tanelerinin incelmesine katkı sağlayarak ultra-ince beynitik yapının oluşumunu ve dayanım özelliklerinde iyileşme sağlamasıdır.

Optimum dayanım-tokluk kombinasyonunu sağlamak için de yapıda martensit oluşturulmasının yanı sıra martensit hacim oranı da önemli bir faktördür. Bu nedenle bu çalışma farklı martensit hacim oranları oluşturularak elde edilen farklı

mikroyapıların analiz edilmesi ve bu yapıların mekanik özelliklere etkisinin incelenmesi hedeflenmiştir.

Bu çalışmada yüksek Si içeren 60SiMn5 çeliğine su verme ve östemperleme ısıl işlemleri ardışık olarak uygulanmıştır. Farklı martensit hacim oranları elde etmek için Ms sıcaklığı tespit edildikten sonra Ms'nin altındaki farklı su verme sıcaklıklarında çeliğe su verilmiş, hemen ardından beynitik yapı oluşturmak için Ms üzerindeki bir sıcaklıkta izotermal işlem yapılmıştır. Ms sıcaklığının tespiti için dilatometrik analiz, ampirik formüller ve JmatPro yazılımı kullanılabilmekle beraber bu çalışmada hesaplamalar JmatPro yazılımı kullanılarak yapılmıştır. Hesaplamaların sonunda Ms sıcaklığı 250 °C olarak belirlenmiştir. Belirlenen sıcaklıklara bağlı olarak ısıl işlem proses tasarımı şu şekilde yapılmıştır: Numuneler 900 °C'de 30 dakika östenitleme işlemine tabi tutulduktan sonra 180, 200, 220 ve 240 °C'de (Ms sıcaklığının sırasıyla 70, 50, 30 ve 10 °C altında) su verme işlemleri yapılmıştır. Bu işlem tuz banyosunda 60 s'de gerçekleştirilmiş ve sonucunda farklı martensit hacim oranlarının elde edilmesi sağlanmıştır. Bu işlemin hemen ardından numuneler 280 °C'de 2 saat boyunca izotermal işleme tabi tutularak martensite ek olarak beynitik yapı da oluşturulmuştur. Elde edilen bu martensitik-beynitik hibrit mikroyapıyı tamamen beynitten oluşturulan mikroyapı ile karşılaştırmak için 900 °C'de 30 dakika yapılan östenitleme işlemini takiben 280 °C'de 2 saat beynitik dönüşüm gerçekleştirilmiştir. Bu işlem de tuz banyosunda gerçekleştirilmiştir.

Yüksek Si içeren çeliğe ardışık olarak uygulanan bu su verme ve östemperleme ısıl işlemlerinin ardından karakterizasyon çalışmaları için mikroyapı incelemeleri, sertlik analizi ve faz hacim oranı analizi yapılmıştır. Mikroyapı incelemeleri optik mikroskop ve SEM ile yapılmış olup, analiz öncesinde uygun şekilde zımparalama, parlatma ve dağlama çalışmaları yapılmıştır. Mikroyapı incelemeleri için ilk etapta herhangi bir ısıl işlem görmemiş parçaya dağlama çalışmaları yapılarak öncül östenit tane boyutu hesaplamaları yapılmış ve öncül östenit tane boyutu ortalama 60 µm olarak hesaplanmıştır. Bu hesaplamalarda optik mikroskoba ek olarak Image J programından da faydalanılmıştır. Bu analizlerinin ardından ısıl işlem uygulanmış numunelere dağlama çalışmaları yapılarak yapıdaki beynitik ve martensitik yapılar incelenmiştir. Martensit ve beynit yapılarına ek olarak yapıda az miktarda tespit edilen kalıntı östenit hacim oranı da belirlenmiştir.

Mikroyapı incelemelerinin ardından numunelere sertlik analizi yapılmıştır. Bu analiz Vickers metoduyla 30 kgf yük altında yapılmıştır. Yapılan analizin sonucunda su verme sıcaklığı 180 °C'den 240 °C'ye arttıkça martensit hacim oranının azalmasına bağlı olarak sertlikte azalma meydana gelmiştir.

Yapıdaki hacim oranının tespiti için X-ışını difraksiyon (XRD) analizi yapılarak kalıntı östenit hacim oranı belirlenmiştir. Yapılan bu analize göre su verme sıcaklığı 180 °C'den 240 °C'ye arttıkça yapıdaki kalıntı östenit hacim oranında doğrusal olmamakla beraber bir artış sağlanmıştır. Kalıntı östenitin hacim oranının tespitinin ardından martensit hacim oranının saptanması için Koistunen Marburger denklemi kullanılmıştır. Yapılan hesaplamalar sonucunda su verme sıcaklığının 180 °C'den 240 °C'ye arttırılmasıyla martensit hacim oranında %53'den %10'a bir azalma meydana gelmiştir. Kalıntı östenit ve martensit hacim oranı hesaplamalarından sonra yapıda kalan diğer yapının beynit olduğunu göz önüne alındığında, su verme sıcaklığı 180 °C'den 240 °C'ye arttırıldığında yapıdaki beynit oranında % 42,8'den % 81,7'ye artış sağlandığı belirlenmiştir.

Farklı hacim oranlarında oluşturulan martensit ve beynitik yapılar karşılaştırıldığında tamamen beynitik yapıda martensit oluşmamasına bağlı olarak sertlik daha azdır. Sertliğe ek olarak çekme , darbe ve yorulma özellikleri de incelenmiş olup; martensitik ve beynitik dubleks mikroyapılı çeliğin akma ve çekme dayanımı tamamen beynitten oluşan mikroyapıya göre daha yüksektir. Bu değerler sırasıyla 1920 MPa, 2050 MPa, 1825 MPa ve 1910 MPa olarak belirlenmiştir. Darbe özelliklerinde ise tamamen beynitten oluşan mikroyapı 33 J darbe direncine sahipken martensit ve beynitik dubleks yapı 10 J darbe direncine sahiptir. Dolayısıyla yapıda beynit oranı arttıkça ve martensit oranı azaldıkça darbe direncinin arttığı tespit edilmiştir. Yorulma özelliklerinde ise diğer mekanik özelliklerde olduğu gibi önemli bir fark tespit edilememiştir.

1. INTRODUCTION

The microstructure of steel strongly depends on the heat treatment procedure. Depending on the cooling rate and quenching type, steel microstructure can vary between pearlite, bainite and martensite. Bainite, which combines both high strength and high toughness, is a common constituent of existing high-strength steels. As a result, it finds utility in a variety of contexts [1]. The creation of a previous phase, such as pre-existing martensite (PM), prior to the bainitic transformation has seen increasing attraction. Furthermore, numerous investigations indicate that martensite-bainite duplex microstructures have superior strength-toughness combinations compared to single martensite or entirely lower bainite microstructures [2,3].

Tomita et al. [4] reported that the martensitic-bainitic duplex 440 steel steel exhibited better qualities in comparison to steel having fully martensite and concluded that steel containing 25% bainite in its structure provides the best combination in terms of strength and toughness.

M.Morawiec et al. [5] investigated the effect of pre-existing martensite on bainitic transformation kinetics in 3% medium-Mn multiphase steel structure and the findings of the study are as follows: bainitic transformation starts and ends much faster with the effect of the presence of martensite within the structure and also they emphasized that the microstructures were predominantly constituted of thin bainitic laths with preserved austenite, together with a tiny quantity of martensitic-austenitic islands, at a temperature of 400 °C.

When the pre-existing martensite's accelaration process are analyzed, it is commonly recognized that martensite preferentially nucleates at austenite-austenite (γ-γ) interfaces, or at prior-austenite grain boundaries [6]. Following quenching, an isothermal treatment stops the athermal martensite production before the transition is completed. This results in the material containing martensite-austenite (α′-γ) interfaces, which may serve as possible sites for nucleation. Increasing the volume percentage of preceding athermal martensite and, consequently, the density of α′-γ interfaces will accelerate the isothermal transition beyond Ms. Nevertheless, the

reasons for this acceleration are not fully known, and it is still uncertain how these α′-γ limits may affect the kinetics of subsequent transformations [5,7,8].

The aim of the this paper is to examine the effect of the martensitic/bainitic dublex steel, which has different volume fractions of prior martensite in the structure, on the change in the width of bainite lats by using SEM and its effect on mechanical properties such as toughness and strength. In addition, there are few studies on the effect of pre-existing martensite on the fatigue properties of martensitic bainitic dublex microstructure steel. In this study, it is also aimed to investigate fatigue properties in addition to microstructure and other mechanical properties.

2. LITERATURE REVIEW

The objective of this chapter is to examine and analyze the existing body of research pertaining to the structures of martensite and bainite. The section including the gathering of data on bainite, martensite, and martensite-bainite duplex structures. It explores their distinctions, various forms, and the methods by which they are formed.

2.1 Martensite

Martensite is a phase that is not stable in the long term and originates from austenite when it is rapidly cooled to low temperatures. As illustrated in Figure 2.1, the crystal structure of martensite, which is produced by quenching the austenite phase in carbon steels, is a body-centered tetragonal (BCT) lattice. This lattice can be regarded as an α lattice with one of the cubic axes elongated [9].

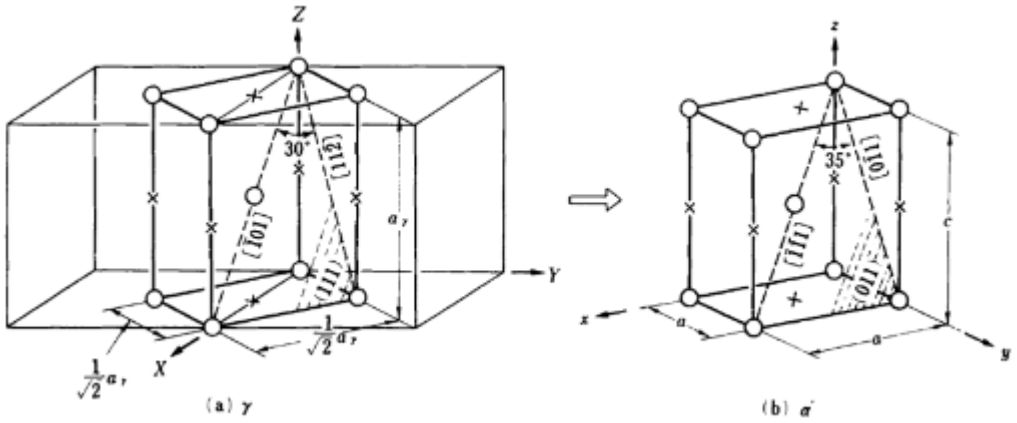

Figure 2.1 : Conversion from γ to α [9].

A rapid cooling rate is required to prevent the formation of any other phase, including ferrite, it is necessary to have a quick cooling rate that avoids the nose of the TTT diagram. The transition of martensite is athermal, meaning it occurs without changes in temperature. The cooling rate required to produce martensite is extremely rapid, preventing any diffusion from taking place. As a result, all the carbon present in the parent austenite becomes trapped in the structure, causing distortion in the austenite lattice [10,11].

2.1.1 Microstructure

Martensite microstructure varies depending on the C content [10]. Lath martensite is generated at elevated temperatures, while thin plate martensite is produced at lower temperatures (Figure 2.2). Lath martensite is generated at elevated temperatures, while thin plate martensite is produced at lower temperatures. An elevation in carbon content results in an increase in the transition temperature of martensite morphology, transforming its structure from a lenticular form to a thin plate configuration [12].

The dimensions of martensite laths are extremely minute, typically ranging from 0.2 to 0.5 μm. Consequently, individual laths are not easily discernible in optical micrographs. Nevertheless, due to the inclination of lath martensites to align in parallel within a significant area of the austenite grain, lath martensite displays a distinctive microstructure when seen under an optical microscope. Steels characterized by a lath martensite microstructure exhibit remarkable toughness, with an approximate yield strength of 1000 MPa. Achieving satisfactory toughness when in the quenched state is feasible due to this combination of elevated strength and the absence of supplementary tempering procedures [10,13].

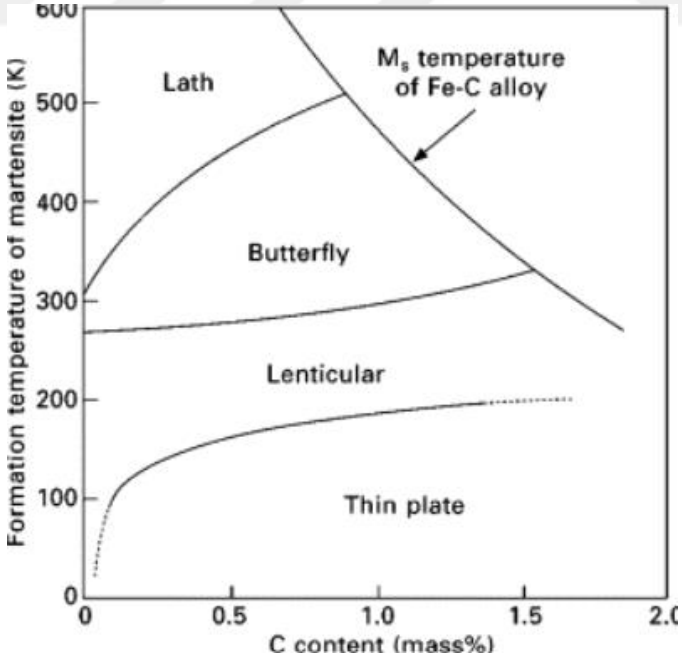

Figure 2.2 : Formation range of various types of martensite [10].

Thin plate martensite is distinguished by its exceptionally smooth and flat interface, without a central ridge. Additionally, the transformation twins in martensite, namely the (112) twins, span throughout the whole distance between the interfaces. When it

comes to α′ martensite with different morphologies, the A/M interface is typically not flat and there are no transformation twins present in the martensite at the interface. In addition, it is typical for the parent austenite near thin plate martensite to have a scarcity of dislocations [10,13].

The transition from austenite to martensite in low alloy steels commences at a temperature, Ms, that is relatively constant and unaffected by lowering rates of up to 50,000 °C/s and this Ms temperature can be determined by using dilatometry, empirical formulas or JmatPro software.

2.2 Bainite

Bainite is a common constituent in contemporary high-strength steels, primarily owing to its remarkable combination of toughness and strength, rendering it highly desirable for various applications. Bainite types are typically divided into lower and upper bainite. Apart from these, Zaica modeling is one of the most well-known schemes proposed by Zajac et al., and in this model, 5 different bainite structures are expressed as shown in Figure 2.3 and in Table 2.1 [14,15].

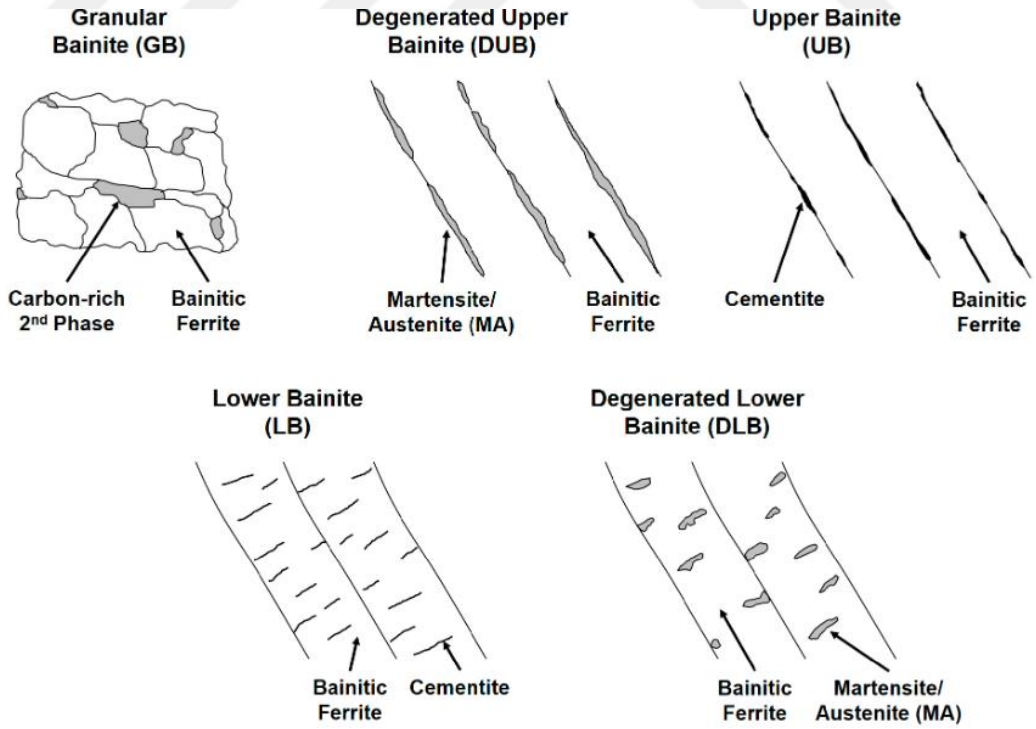

Figure 2.3 : Bainite types [14].

Table 2.1 : Classification of bainite types [15].

Classification	Ferrite morphology	Second phase type
Granular bainite	Irreguler	Transformation product from carbon rich austenite: pearlite, cementite,bainite,MA,martensite.
Upper bainite	Lath-like	Coarse cementite precipitated into lath boundaries + finely dispersed intralath carbides.
Degenerated upper bainite	Lath-like	M-A microconstituents along lath boundaries.
Lower bainite	Lath-like	Cementite precipitated inside laths at 60° incline to lath direction
Degenerated lower bainite	Lath-like	Intralath M-A constituents

Bainite, similar to martensite, is classified as a non-equilibrium structure due to its formation through comparatively rapid cooling processes in contrast to equilibrium phases. The rate of cooling is sufficiently swift to prevent the formation of pearlite, but not swift enough to generate martensite. It is formed at temperatures between Ms and the range of temperatures required for the pearlite transmutation [15,16].

Whereas cementite particles are distinguished by their fine and coarse texture, bainitic ferrite has a needle-like structure similar to martensite laths. When compared to pearlite, bainite is stronger and harder because to the highly refined blend of ferrite and cementite that it contains. Figure 2.4 illustrates discernible alterations in various microstructure [17].

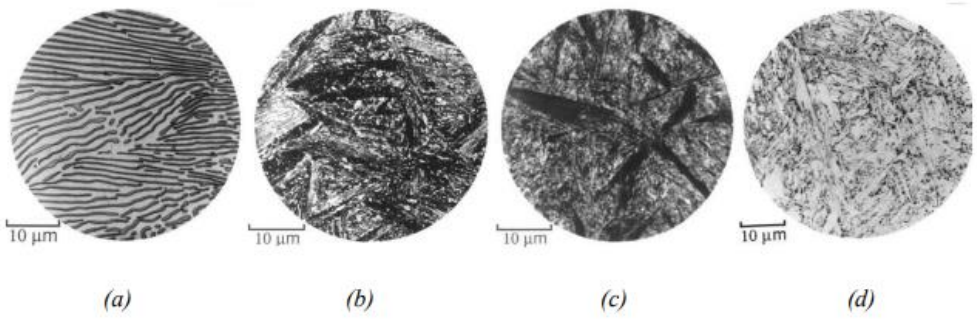

Figure 2.4 : Microstructure of the steel (a) pearlite, (b) bainite, (c) bainite, (d) martensite [17].

Upper bainite's microstructure is made up of tiny ferrite plates, each measuring around 10 µm in length and 0.2 µm in thickness. Sheaves are the groupings in which the plates develop. Every sheaf has parallel plates with the same crystallographic orientation and distinct crystallographic habits. As shown in Figure 2.5, the separate plates inside a

sheaf are sometimes referred to as the "sub-units" of bainite. Cementite particles, austenite, or low-misorientation borders are often used to divide them. The isothermal formation of upper bainite occurs at elevated temperatures in comparison to lower bainite. Situated slightly below the pearlite transmutation zone, the average temperature falls within the interval of 400 °C to 550 °C [15].

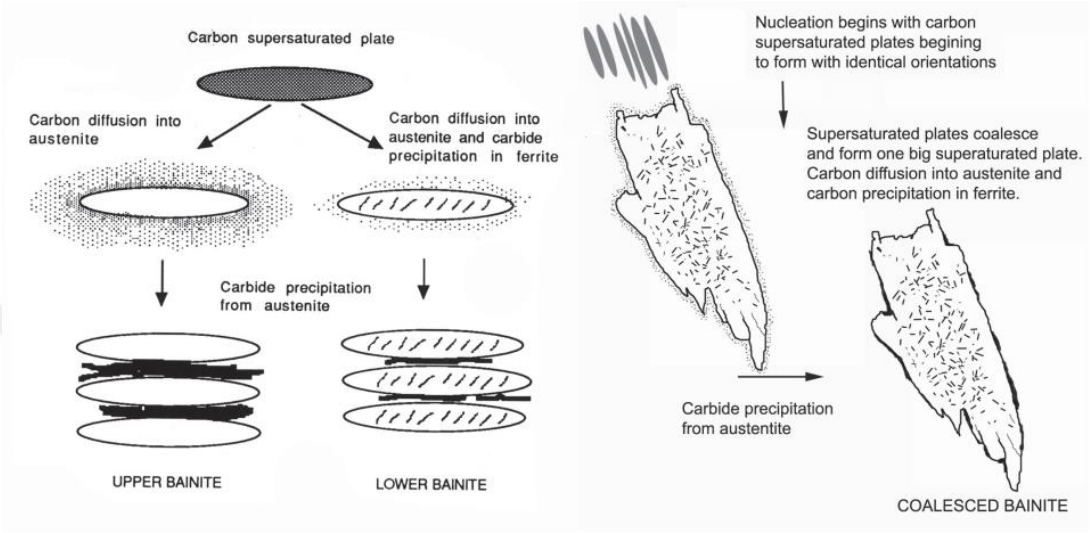

Figure 2.5 : Upper and lower bainite figures [17].

2.3 Martensitic-Bainitic Mutiphase Microstructure

The martensite/bainite multiphase microstructure exhibits superior strength-toughness correlation in comparison to the conventional martensitic microstructure. In recent studies, in order to generate martensite-bainite duplex microstructures, two techniques have been utilized: one involves isothermal holding below Ms temperature and the other involves introducing a specific fraction of pre-existing martensite prior to bainite transformation. The other method involves producing lower bainite by isothermal holding at a temperature above Ms after first pre-quenching martensite at a temperature below Ms to obtain a certain proportion of prior martensite.

Pre-existing martensite has been shown to accelerate future bainite nucleation, according to the majority of current research that examine its effect on the nucleation kinetics of subsequent bainite transition [3,18].

Lu et al. [3] studied GCr15 bearing steel, where toughness and strength are especially important. They investigated the effect of the martensite pre-quenching process on the kinetics of the bainite transformation in bearing steel. The results showed that pre-

existing martensite greatly faster than the formation of bainite compared to direct bainite austempering. Furthermore, in the early development stage, the bainitic transformation rate after prior quenching of martensite is faster than that of direct bainite austempering, and this rate decreases when the martensite pre-quenching temperature decreases. At the end of this research, the results demonstrated that the tensile strength of samples subjected to heat treatment, specifically martensite pre-quenching at 200 °C followed by bainite transformation at 240 °C, increased significantly from 43 J to 71 J in comparison to samples that were conventionally quenched and tempered (QT). Additionally, there is a minor reduction in tensile strength from 2170 MPa to 2143 MPa.

In addition to this study, similar studies were conducted on spring steels, which is a material group where toughness is important. The following findings were obtained in this study, the following findings were obtained by systematically examining the influencing qualities along with mechanical property variations based on lath length and width were thoroughly investigated, yielding the following findings::The width of the bainite laths in the quenched and tempered sample is smaller compared to the directly austempered sample, measuring 0.81 micrometers and 1.76 micrometers, respectively, and also as for tensile strengths of quenched and tempered and direct austempered samples are measured at 1723.1 MPa and 1824.4 MPa. These values are 73.8% and 84% higher than the non-heat treated samples, respectively [19,20].

As a result, the effects of the martensitic-bainitic duplex structure that is generated on the microstructure are shown in Figure 2.6, according to an examination of numerous studies. In this schematic diagram, when quench and tempering are done, prior martensites are formed in the microstructure, which is different from the situation where direct austempering is done. These prior martensite form nucleation points for the bainite to be formed subsequently. This accelerates the process and allows getting a finer bainite structure by lowering the width of the laths, which is crucial in the bainite mechanism. In this case, it contributes to the improvement of mechanical properties.

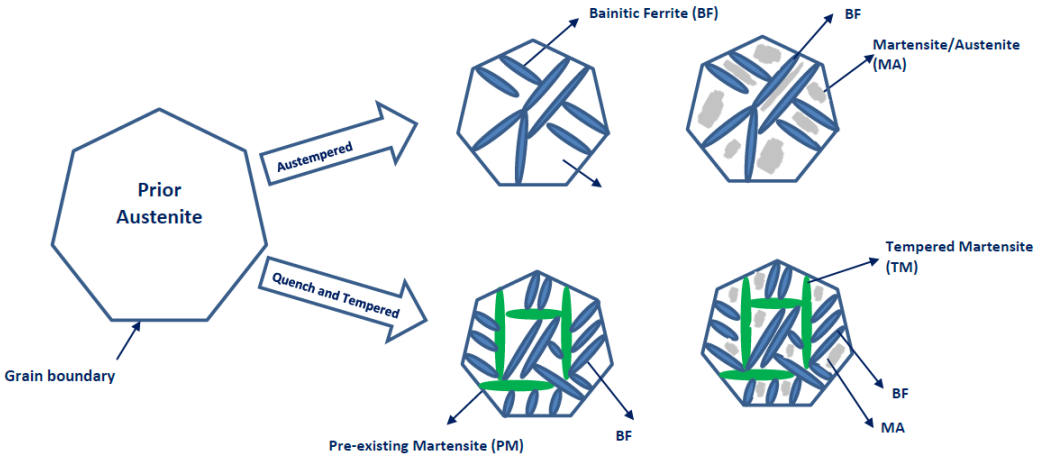

Figure 2.6 : Schematic diagram of direct austempering and quench and tempered process respectively [19].

2.4 60SiMn High Silicon Spring Steel

The primary criteria for spring steel are a high yield strength and high fatigue strength. Springs are manufactured using several types of materials, including carbon steels, silicon steels, manganese steels, silicon-manganese steels, and stainless steels, according on the specific application requirements [21]. Typically, the spring steel has a relatively high amount of Si to prevent the development of carbides when it is tempered. As a result, the steel exhibits strong resistance to void formation and cleavage fracture [19,22].

The effective way is the chemical composition in order to enhance the mechanical properties of spring steel but is being alone is insufficient and in addition to chemical composition selection of the effective heat treatment procedure improve the mechanical properties of these steels [23].

The spring steel produced through the quenched and tempered process ultimately displays a tempered martensite microstructure. Nevertheless, the phenomenon of hydrogen embrittlement and cracking is inevitable when enhacing its strength. Delayed hydrogen embrittlement in spring steel results in a substantial reduction in fatigue strength owing to the fragility of grain boundaries. Consequently, it is expected that replacing the final microstructure of the spring steel with a mixed structure comprising bainite instead of martensite will improve its mechanical properties as shown in Table 2.2 [20].

Table 2.2 : Mechanical properties of 60SiMn5 steel properties [20].

Properties	Value
Yield Strength (MPa)	>1000
Tensile Strength (MPa)	>1100
Elongation at fracture (%)	15

3. EXPERIMENTAL METHODS

This section of this study includes the details of material, heat treatments processes, microstructural examination and mechanical test equipments.

3.1 Materials

In the experimental studies, 60SiMn5 alloy steel was used and its chemical composition is given in Table 3.1.

Table 3.1 : Chemical composition of 60SiMn5 steel.

Element	Composition (wt.%)
C	0.65
Si	1.14
Mn	1.00
S	0.001
P	0.006
Cu	0.04
Ni	0.04
Mo	0.01
Cr	0.07

3.2 Heat Treatment Procedures

In the determination of Ms temperature of the steel, Jmat-Pro software, an emphrical formula known as Andrew equation, dilatometry were used. Before starting the heat treatment processes, the Ms temperature was determined from the TTT diagram constructed by Jmat-Pro software.

3.2.1 Process design

In order to examine different martensite volume fractions in the microstructure, different quenching temperatures below the Ms temperature such as 180, 200, 220, 240˚C was selected for quenching. In addition to these, to compare the martensitic-bainitic duplex structure with different martensite volume fractions and the completely

lower bainitic structure, the steel was austempered at 280 °C, which is above Ms temperature. A spesific steps of the procedure were as follows: Firstly, the prepared samples were placed in a Protherm muffle furnace embedded in iron filings to prevent oxidation and decarburization. The temperature was increased to 900 °C austenization temperature and the samples were held at this temperature for 30 minute. After this process the samples were quickly removed from the furnace and placed into salt balt furnace below the Ms temperature 180, 200, 220, 240 °C. The samples were held for 1 minute in order to obtain martensitic microstructure. After the quenching, the samples were transferred the etuv at 280 °C, and held at this temperature for 2 h for bainitic transformation. Also to make a comparison, fully lower bainitic structure was produced by holding he samples at 280 °C for 2 h just after the austenitization.

3.2.2 Heat treatment equipments

The austenization process was carried out in Protherm muffle furnace. Pre-quenching process was carried out in a salt bath containing AS 135 annealing salt. Isothermal heat treatments were conducted in etuv (Figure 3.1).

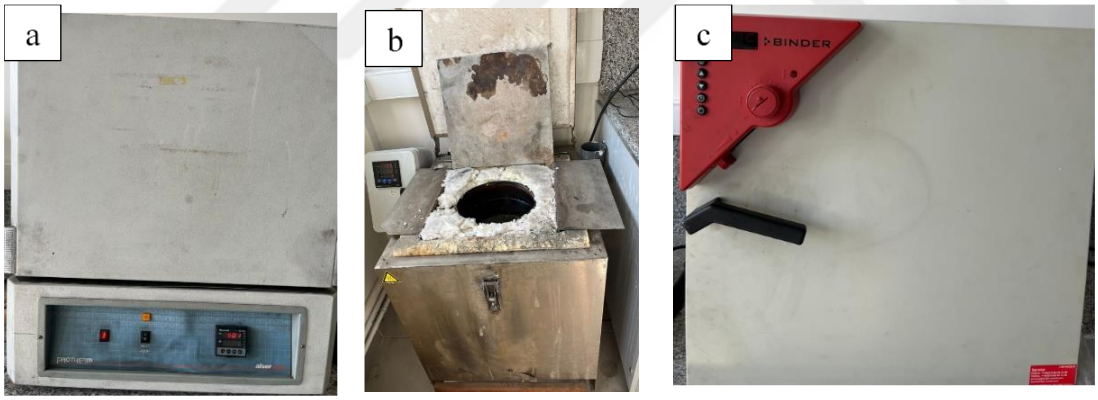

Figure 3.1 : Heat treatments equipments a) Protherm muffle furnace, b) Salt bath c) Etuv.

3.3 Microstructural Characterization and Fractography

Microstructural analysis was performed by using cubic samples with dimensions of 10 x10 x10 mm^3. As-received and heat treated samples were cut into this dimension by a Metkon precision diamon cutter equipment. After the samples were mounted in bakelite, thete were ground by using sand papers from 120 to 2500 mesh. After grinding, the samples were polished with 6 μm and 1 μm of Metkon polycrystalline diamond suspensions. The as-received samples were etched at 80 °C for 25 s by a

solution consisting of 50 ml water, ¼ tea spoon teepol ($C_{18}H_{29}NaO_3S$), 0.5 gram picric acid, and 1 drop HCl to reveal prior austenite grain boundaries. The heat treated samples were etched by 4 vol. % Nital solution. The etched sanples were examined by Nikon optical microscope and SU500 Scanning Electron Microscope (SEM). Fractography characterization of the fractured samples was conducted on the same SEM.

3.4 Mechanical Characterization

3.4.1 Hardness testing

The hardness test was performed using a Vickers hardness tester with a test load of 30 Kgf (HV30). At least five measurements were taken from each sample, and the results were averaged.

3.4.2 Tensile testing

Tensile test samples were machined from the rectangular steel blocks by a computer numerical control (CNC) lathe according to ASTM E8 standard. The dimensions of the tensile test specimen are given in Figure 3.2. The tensile test was conducted at a cross head speed of 1 mm/min using a Shimadzu AG-IC model electromechanical universal testing machine with a load cell of 100 kN. For each heat treatment, two samples were tested. prepared. Yield strength, and ultimate tensile strength and elongation at fracture were acquired from the tensile tests.

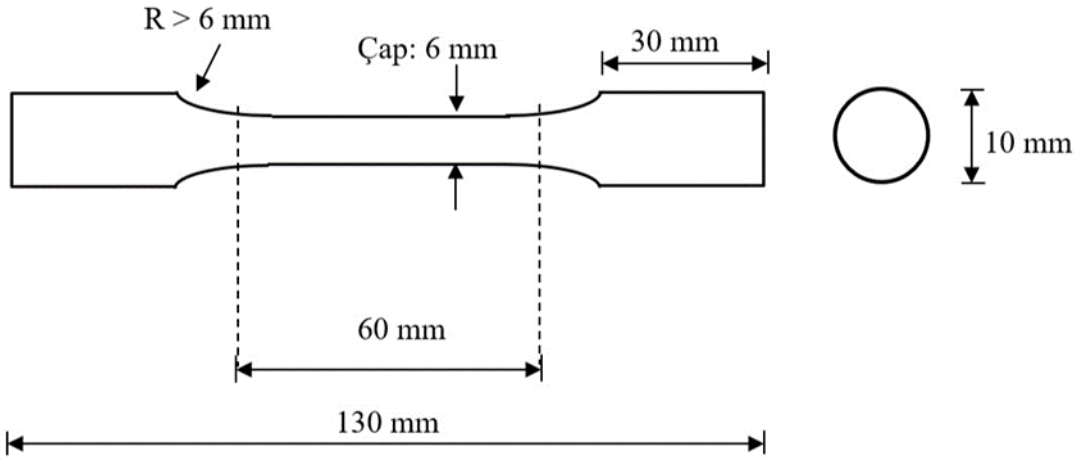

Figure 3.2 : Geometry of tensile test samples.

3.4.3 Impact testing

Impact tests were conducted using Charpy impact tester with a capacity of 300 J. V-notched samples with the dimensions of 55 mm (L) x 10 mm (W) x 10 mm (T) were machined in accordance with ASTM E 23 and a standard. For each condition 3 samples were tested, and the resuts were averaged.

3.4.4 Fatigue testing

Hourglass fatigue test samples with a continiuous radius in the gage section were machined according to ISO 1143 standard. Gage diameter and length were 6 mm and 35 mm, respectively (Figure 3.3).

After the heat treatment procedure, the fatigue test samples were manually polished to provide a smooth surface.

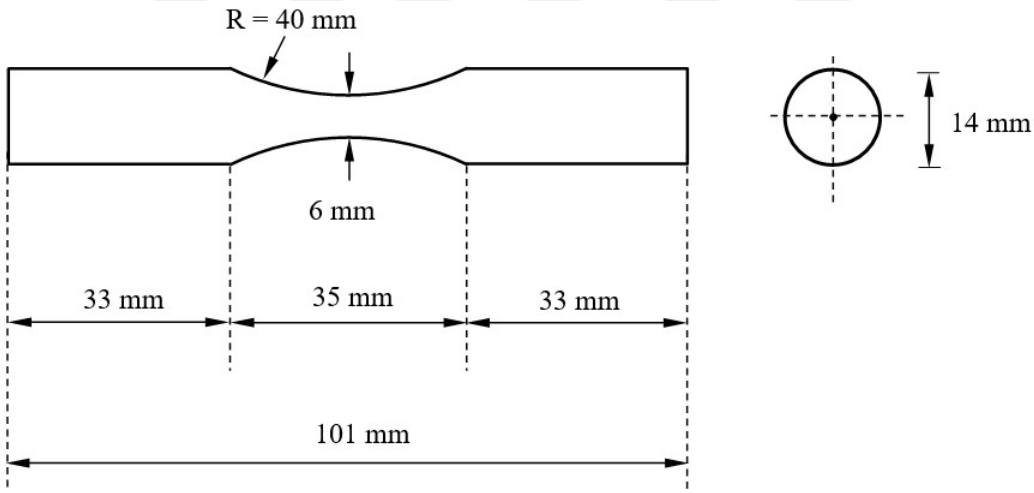

Figure 3.3 : Geomtry of fatigue test samples.

High cycle rotating bending fatigue tests were conducted on Walter & Bai rotating bending fatigue tester (Figure 3.4). It allows bending the samples in four point loading configuration by the application of dead weights. Accordingly, the samples were subjected to succesive tensile and compressive stresses along its length. The stress ratio was R = -1. The stress amplitude was calculated by Eq. (3.1) as follows

$$\sigma = \frac{32M}{\pi D^3} \tag{3.1}$$

where

σ = Stress amplitude (MPa),

M = Bending moment (N-m) (500.F),

The moment arm length is 500 mm,

F = Load (N)

D = diameter of the sample (mm).

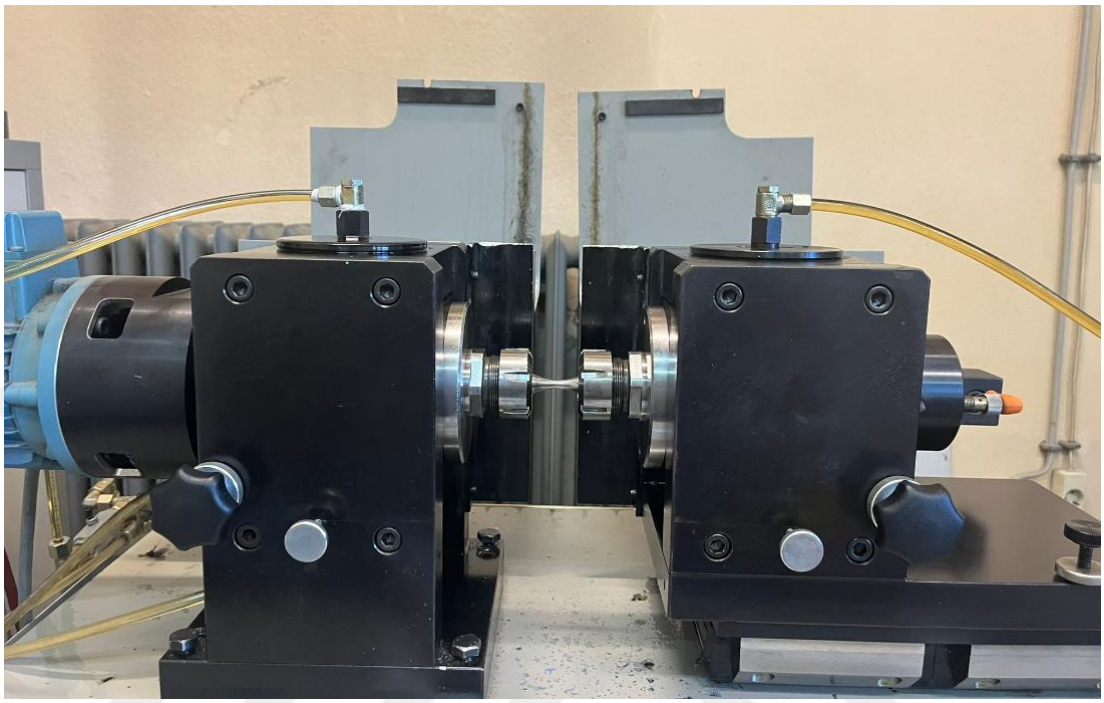

Figure 3.4 : Rotating bending fatgue test machine.

4. RESULTS AND DISCUSSION

In this chapter of the thesis study, the results of the characterizations specified in the experimental part are given.

4.1 TTT Data

Ms temperature was calculated by using the empirical formula and Jmat-Pro software, taking the chemical composition given in Table 3.1. Dilatometry measurements was also used, and the results were evaluated. As a result of the evaluations, it was determined that the literature studies, the results of Jmat-Pro software and the empirical formula were close to each other and it was decided to determine the Ms temperature as 250 °C and the heat treatment process design was created taking this temperature into consideration.

Table 4.1 : Ms temperature calculations according to different methods.

Method	Ms Temperature (°C)
Emprirical Formula	240 ± 5
JmatPro Software	249
Dilatometry	262
Literature Review	250

Additionally, TTT diagram of the 60SiMn5 steel (Figure 4.1) was constructed by JmatPro by using chemical composition given in Table 3.1. Austenization temperature of the steel were selected as 900 °C.

According to the TTT diagram the heat treatment processes are also indicated in Figure 4.2. The detailed process parameters are shown in the Table 4.2.

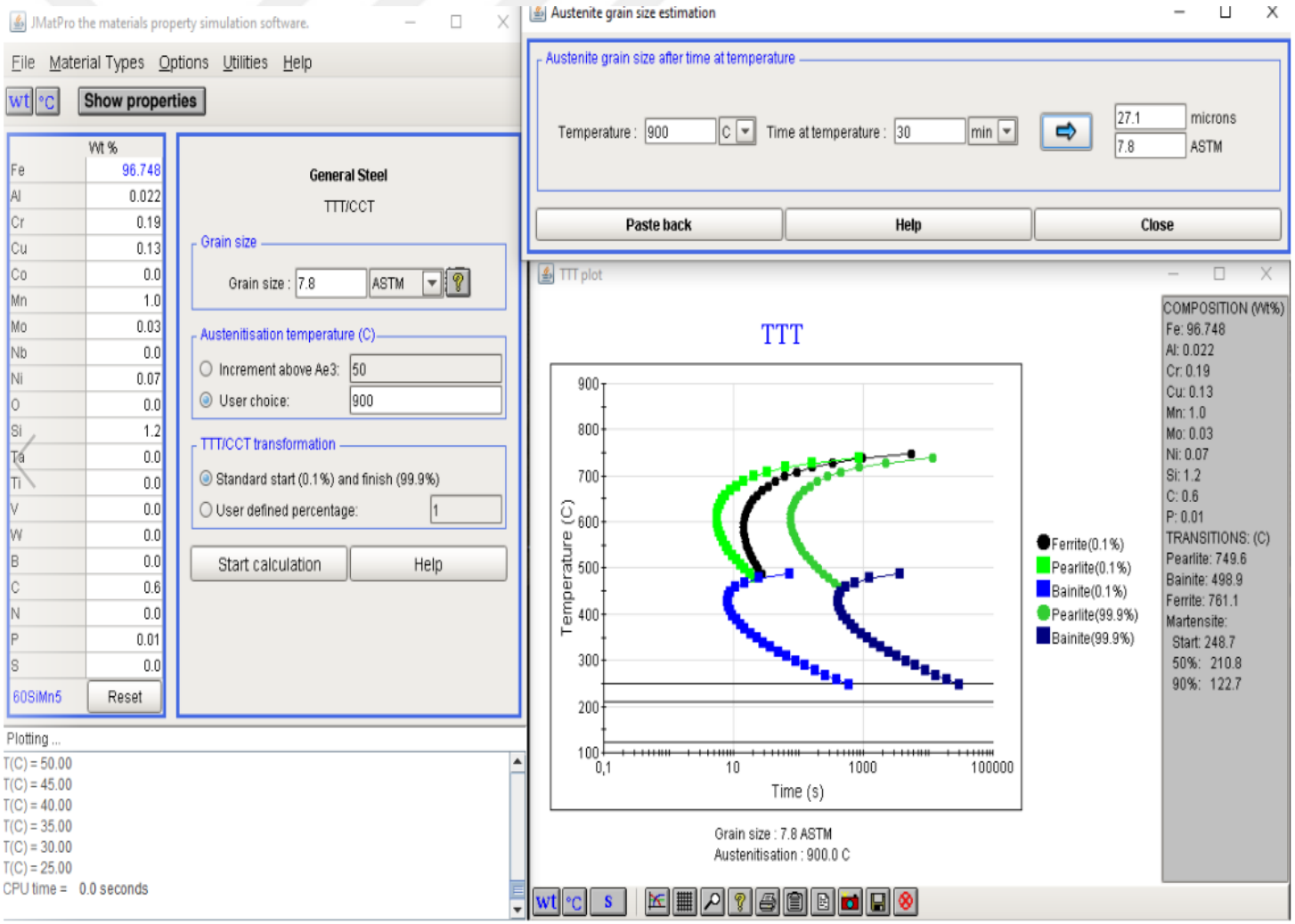

Figure 4.1 : TTT diagram of 60SiMn5 steel.

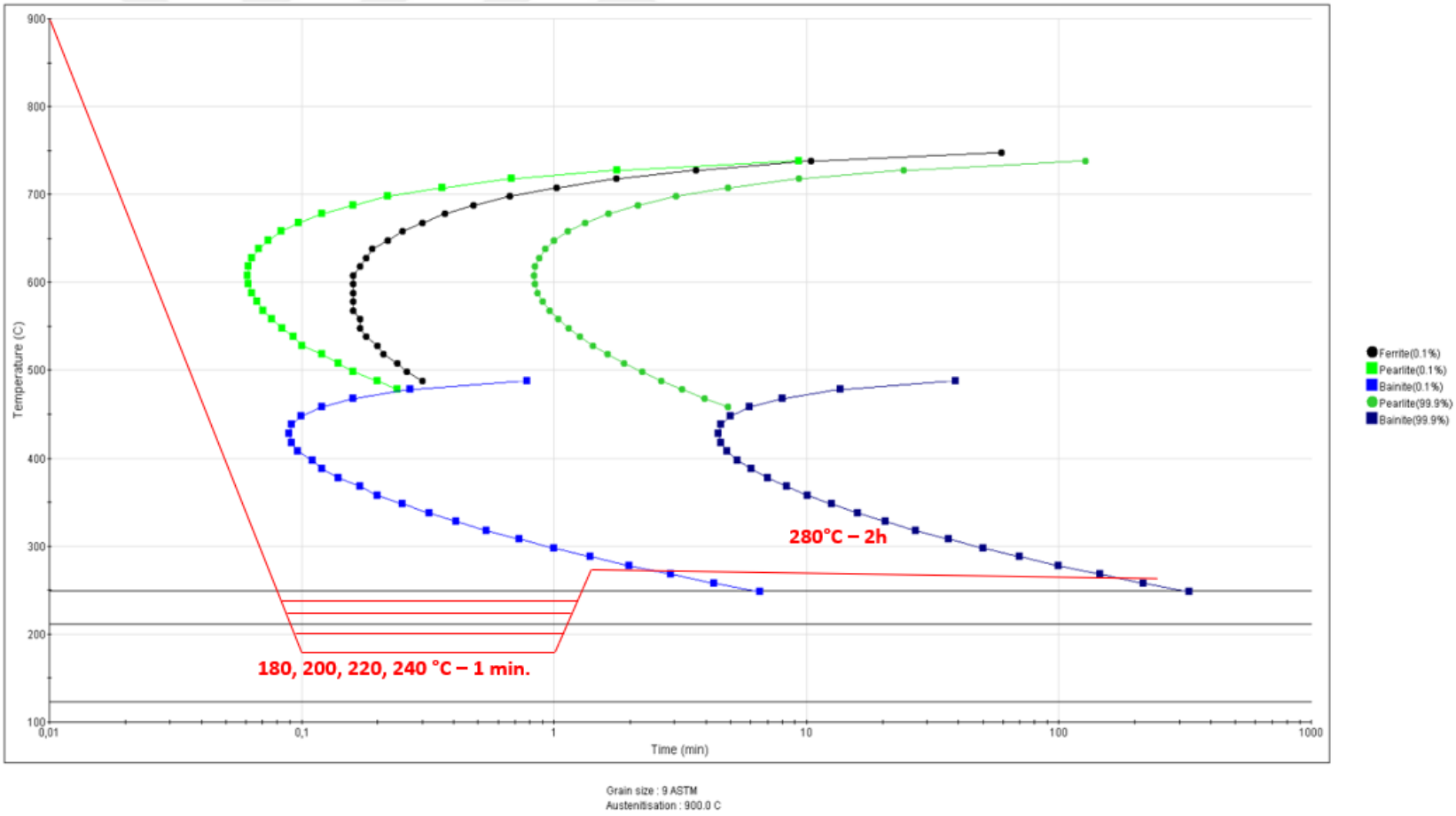

Figure 4.2 : Heat treatment process design of 60SiMn5 steel samples.

Table 4.2 : Heat treatment process parameters.

Process	Austenization Temperature (°C)	Quenching Temperature (°C)	Quenching Hold Time (s)	Bainitic Transformation Temperature (°C)	Bainitic Temperature Hold Time (h)
QBT 180	900	180	60	280	2
QBT 200	900	200	60	280	2
QBT 220	900	220	60	280	2
QBT 240	900	240	60	280	2
DIT 280	900	-	-	280	2

4.2 Microstructural Characterization

4.2.1 As-received sample characterization

Figure 4.3 shows optical micrograph of as-received sample. The martensite volume fraction is significantly affected by carbon concentration, prior austenite grain size and the alloy composition. Steel hardenability is associated with all three parameters [24].

Figure 4.3 : Optical micrograph as-received sample.

After etching trails between 10 and 30 s, prior austenite grain boundaries were revealed, and prior austenite grain size of the steel was estimated by using Image J software as 60 ± 15 µm.

4.2.2 Heat treated sample characterization

Figure 4.4 to Figure 4.7 show optical micrographs of the austempered samples after quenched at different temperatures. Martensite is the dominant phase in the microstructures. Bainite is noticed from its feathery appearance, and relatively small amount of retained austenite was also evident as the white etched phase. It was also noted that bainite nucleation starts from the grain boundaries. As the quenching temperature was increased from 180 °C to 240 °C, martensite volume fraction decreased, as expected, and feathery bainite morphology becomes more apparent.

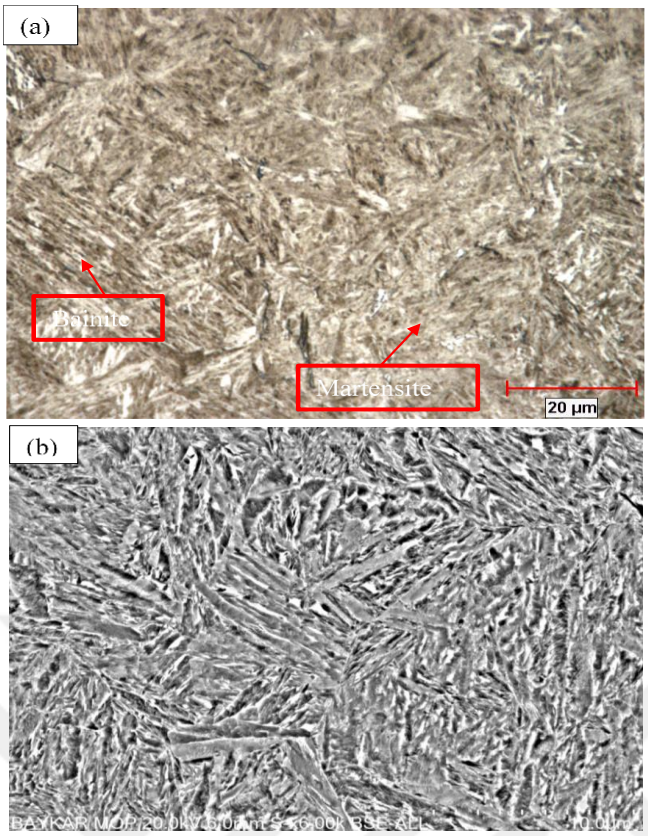

Figure 4.4 : (a) Optical micrograph of QBT 180 sample and (b) SEM micrograph of QBT 180 sample.

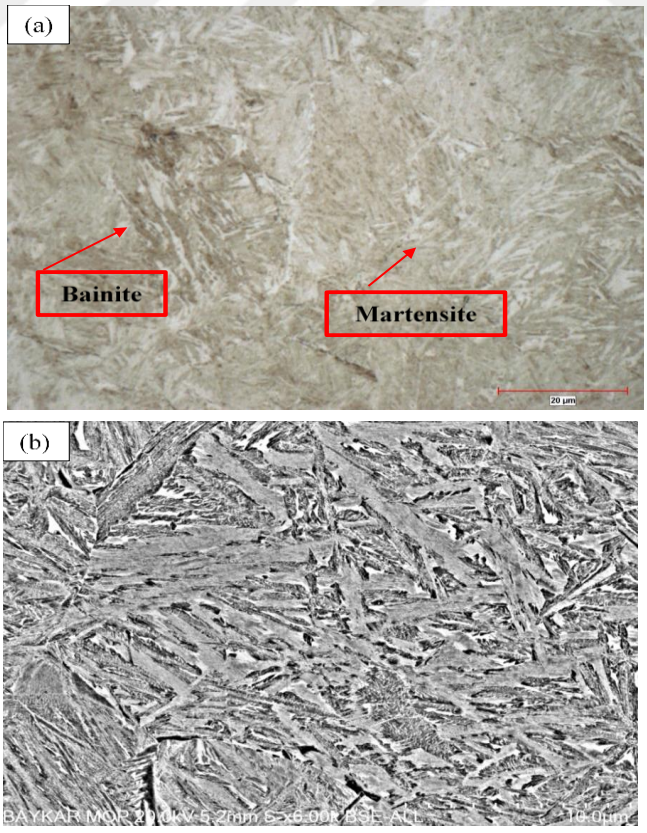

Figure 4.5 : (a) Optical micrograph of QBT 200 sample and (b) SEM micrograph of QBT 200 sample.

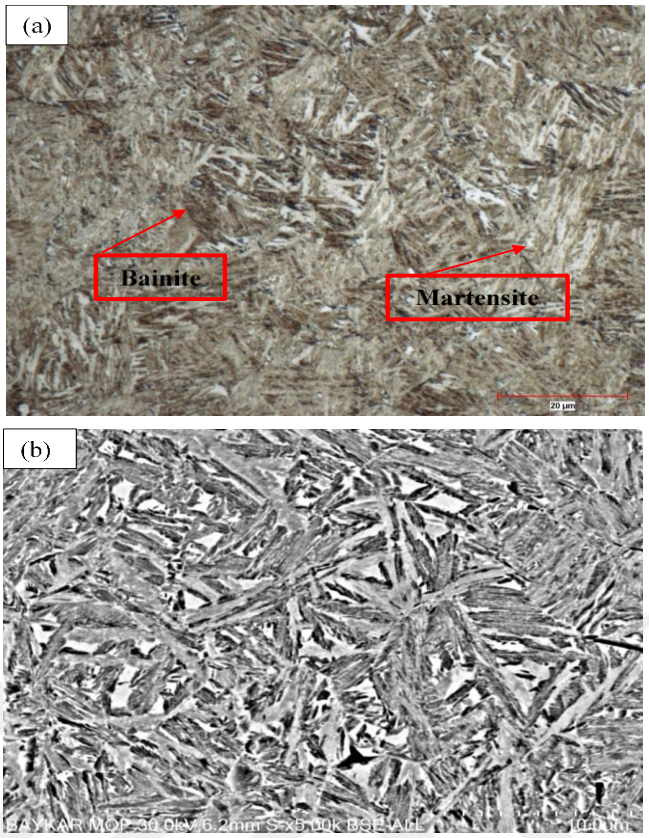

Figure 4.6 : (a) Optical micrograph of QBT 220 sample and (b) SEM micrograph of QBT 220 sample.

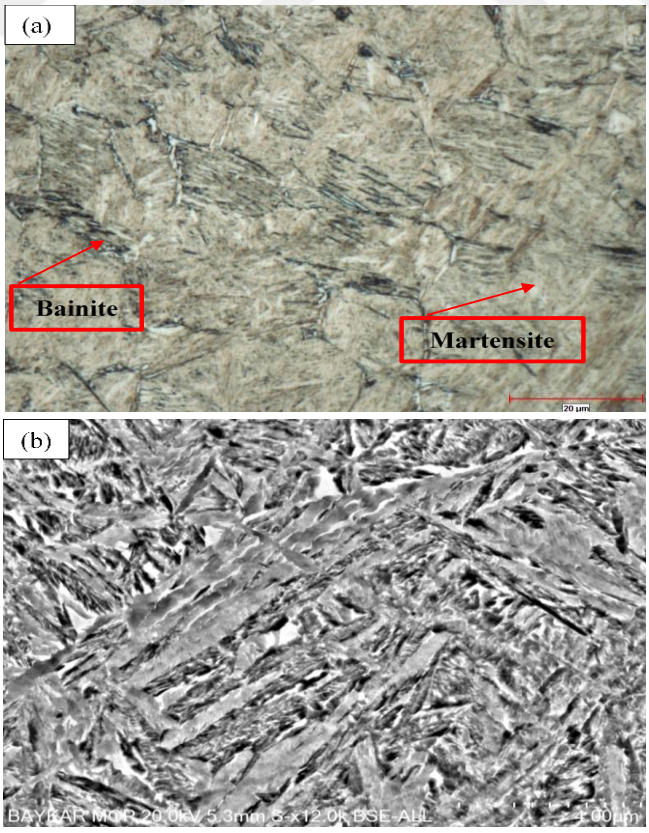

Figure 4.7 : (a) Optical micrograph of QBT 240 sample and (b) SEM micrograph of QBT 240 sample.

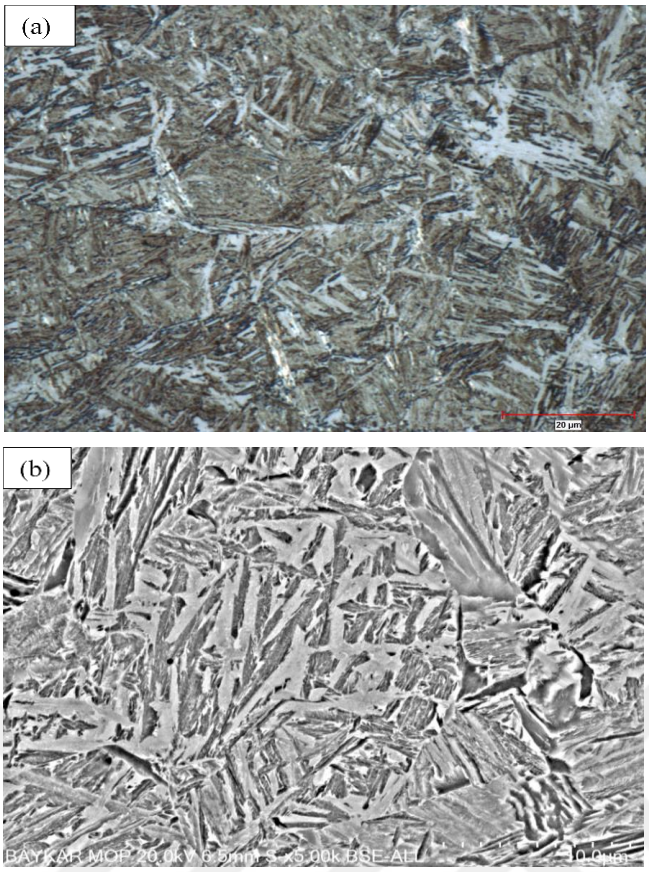

Figure 4.8 : (a) Optical micrograph of DIT 280 sample and (b) SEM micrograph of DIT 280 sample.

4.3 Volume Fraction Characterization

Retained austenite volume fraction was estimated by Eq. (4.1) according to ASTM E 975 standard based on XRD analysis (Figure 4.9). The tesuts of ths analysisi was given in Table 4.3.

$$V_\gamma = \frac{\left(\frac{I_\gamma}{R_\gamma}\right)}{\left[\left(\frac{I_\alpha}{R_\alpha}\right)+\left(\frac{I_\gamma}{R_\gamma}\right)\right]} \tag{4.1}$$

I_α and I_γ: Intensity of ferrite and austenite peaks, respectively.

R_a and R_γ: Correction factor of ferrite and austenite, respectively

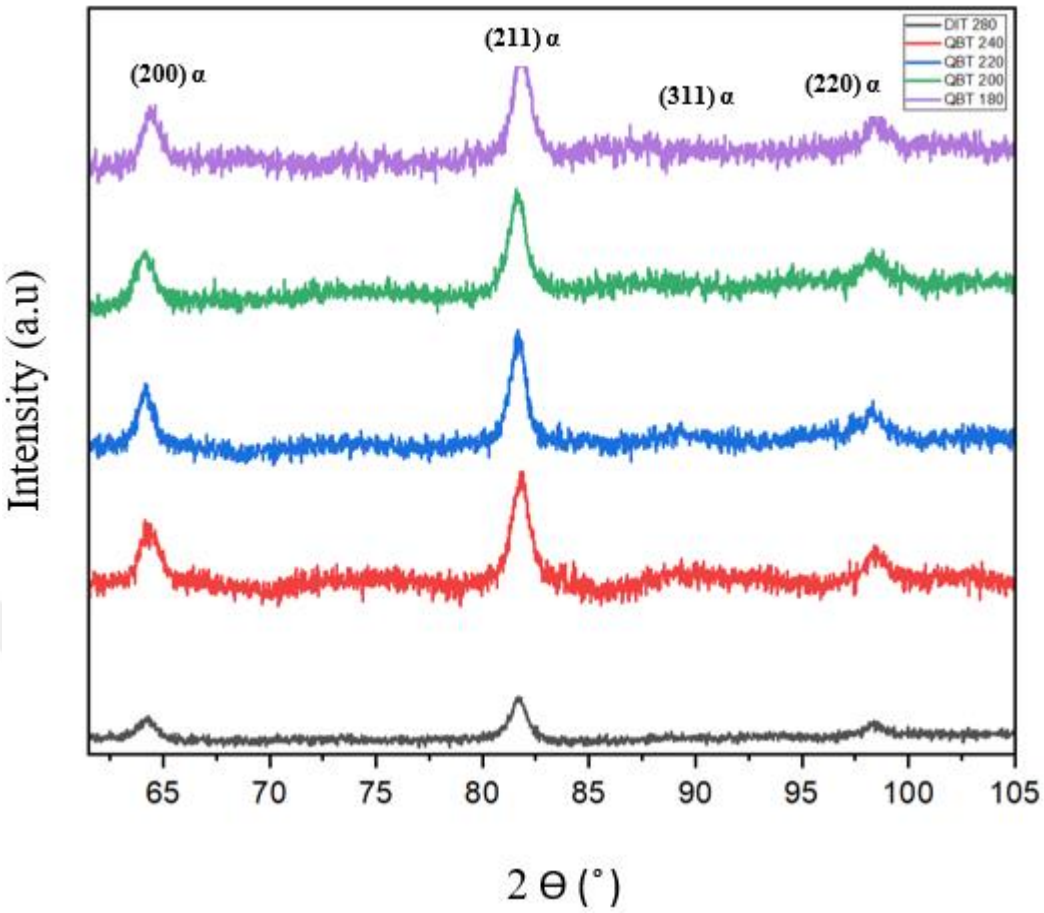

Figure 4.9 : XRD pattern of the samples.

Table 4.3 : Volume fraction of retained austenite.

Process	%Retained Austenite
QBT 180	4.2
QBT 200	3.8
QBT 220	7.5
QBT 240	8.3
DIT 280	6.7

Volume fraction of retained austenite was in the range of 3.8 to 8.3%, and exhibited an increasing tendency with the increase in the quenching temperature. After volume fraction of retained austenite was estimated, pre-existing martensite volume fraction was determined according to Koistunen Marburger equation shown in Eq. (4.2). Remaining portion of the microstructure was assumed to be bainite. Volume fraction of all microstructural constituents are listed in Table 4.4. In the lowest quenching temperature, martensite volume fraction reach 53% of the microstructure, and increasing quenching temperature results in a decrement in martensite volume fraction

to 10%. Correspondingly, bainite volume fraction shows a steady increment from approximately 43% to 82% with the increasing in quenching temperature.

$$\ln(1 - y) = \alpha(Ms) - T \quad (4.2)$$

where

y= Martensite volume fraction,

Ms = Martensite start temperature,

T = Quenching temperature

$\alpha = -1.10 \times 10^{-2}$

Table 4.4 : Volume fraction of retained austenite, martensite, and bainite (%).

Process	Retained Austenite	Martensite	Bainite
QBT 180	4.2	53	42.8
QBT 200	3.8	42	54.2
QBT 220	7.5	20	72.5
QBT 240	8.3	10	81.7
DIT 280	6.7	-	93.3

Figure 4.10 shows the variation of martensite volume fraction for each process. As the quenching temperature incerases from 180 °C to 240 °C, martensite volume fraction decreasses.

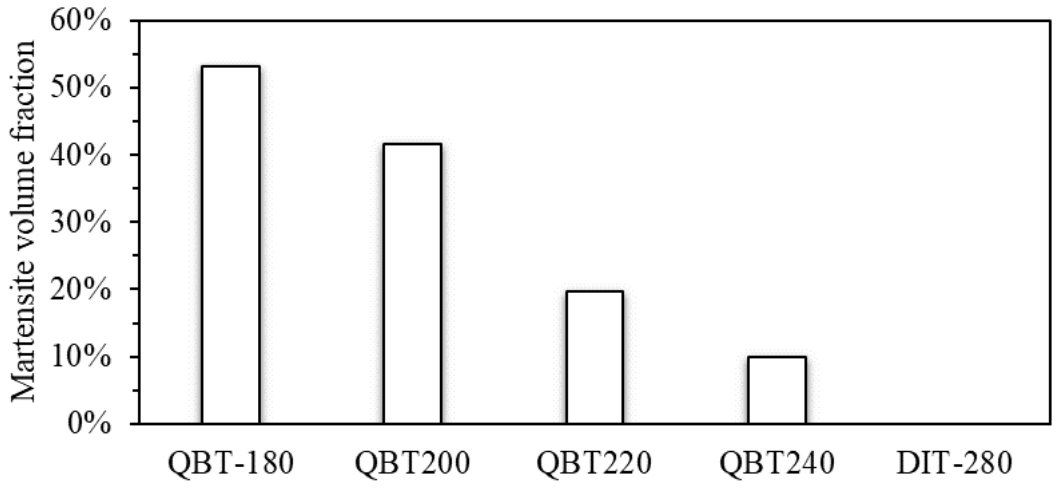

Figure 4.10 : Variation of martensite volume fraction for each process.

4.4 Mechanical Characterization

4.4.1 Hardness testing

Table 4.5 and Figure 4.11 show the variation of the hardness for each process. As the quenching temperature incerases from 180 °C to 240 °C, the hardness of the samples are reduced from 615 HV to 580 HV. All pre-quenched samples have higher hardness than DIT 280 samples which was directly austempered at 280 °C for 2 h just after the austenitization.

Table 4.5 : Hardness of pre-quenched and austempered samples.

Process	Hardness (HV30)
QBT 180	615 ±2
QBT 200	593 ±1
QBT 220	588 ±1
QBT 240	579 ±2
DIT 280	548 ±1
As-received	286 ± 4

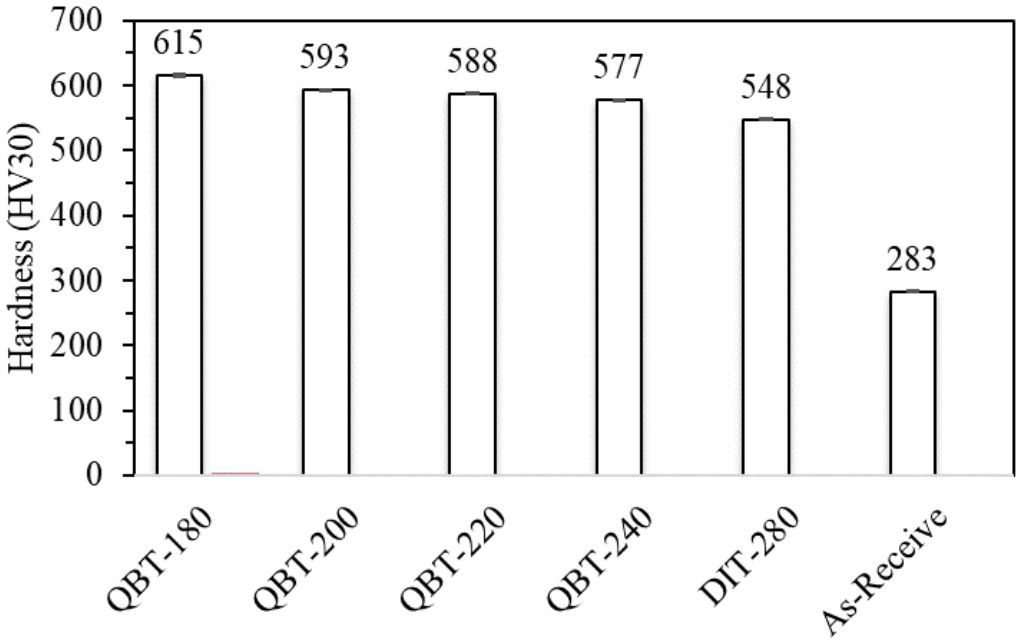

Figure 4.11 : Hardness variation of the samples.

4.4.2 Tensile Testing

Table 4.6 lists the tensile test results, which were taken from stress-stroke strain curves given in Figure 4.12. When the samples with and without heat treatment were compared, the yield and tensile strength increased by more than 2 times while a significant decrease in elongation at fracture was also detected. When the tensile test results of the martensite-bainitic structure (QBT 200) obtained by heat treatment and the fully bainitic structure (DIT 280) are compared, yield and tensile strength of the QBT 200 samples are higher than those of DIT 280 samples.

Table 4.6 : Tensile test results of as-received, QBT200 and DIT280 samples.

Process	0.2% Yield Stregth (MPa)	Ultimate Tensile Strength (MPa)	Elongation at fracture (%)
As-Received_1	590	1003	15.5
As-Received_2	587	982	15.7
QBT200_1	1935	2017	6.1
QBT200_2	1920	2052	6.8
DIT 280_1	1720	1780	5.8
DIT 280_2	1825	1910	5.2

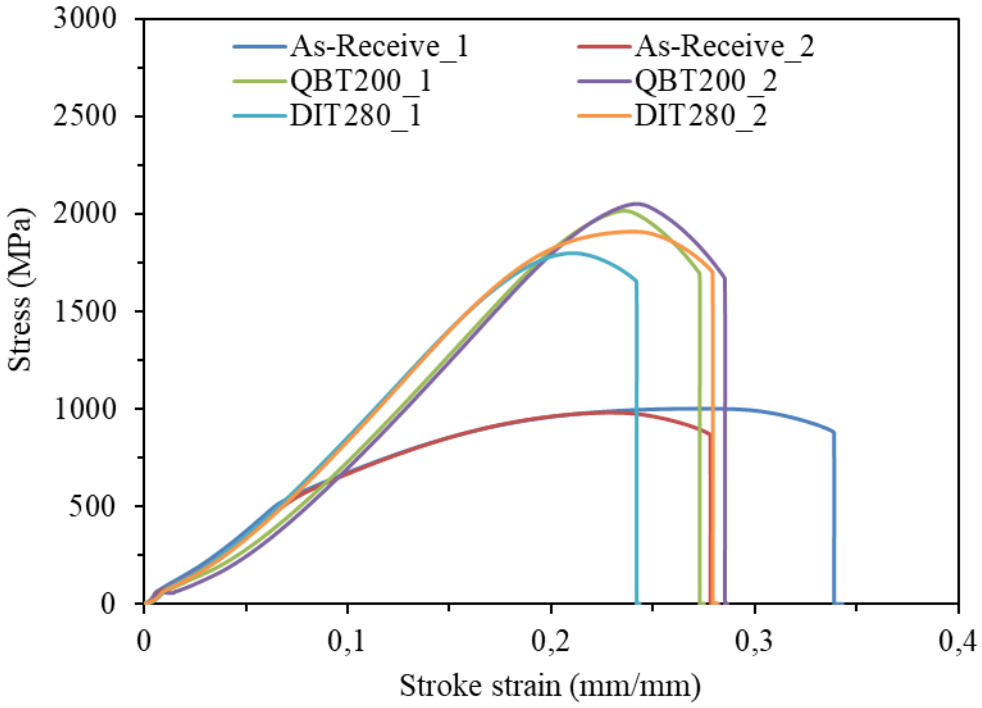

Figure 4.12 : Stress strain curves of the samples.

4.4.3 Impact test results

Impact test results are shown in Table 4.7 and in Figure 4.13 for each processes applied. Impact energy of the DIT 280 samples are higher than those of QBT samples (dublex microstructure). As bainite in the microstructure increases, toughness correspondingly increases. Therefore, maximum impact energy was obtained in the DIT 280 sample, which was subjected to austempering without pre-quenching.

Table 4.7 : Impact test results of 60SiMn5 samples.

Process	Impact Energy (J)
QBT 180	12.09 ± 2
QBT 200	10.46 ± 1
QBT 220	11.11 ± 3
QBT 240	9.15 ± 0.5
DIT 280	33.34 ± 15
As-Received	23.86 ± 4

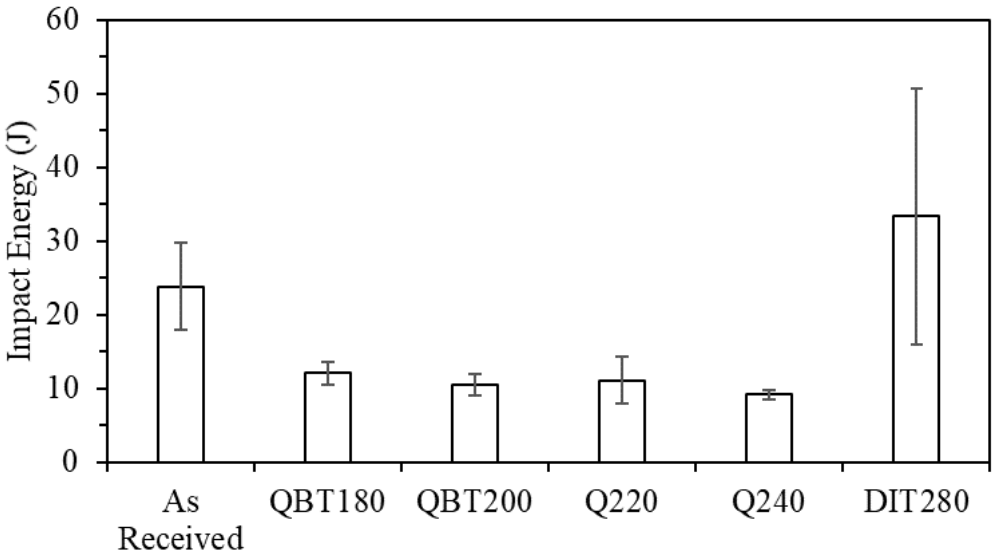

Figure 4.13 : Variation of impact energy for each process.

Additionally the area under the stress-strain curves obtained from the tensile tests also represents toughness. However, considering this area as shown Figure 4.12 and the data obtained from direct impact test result are not compatible with each other. Although the DIT 280 sample shows the highest toughness in the impact tests, the area under the stess strain curve is smaller than the area of the QBT 200 sample.

4.4.4 Fatigue test results

Fatigue test data of the samples are given in Table 4.8. Further, S-N curves of the samples are shown in Figure 4.14. In the fatigue tests, the stress amplitude was chosen between 300 and 600 MPa. Considering the highest stress amplitude, this value corresponds to 33% of the average yield strength of the samples. It was determined that the number of cycles increases as the stress amplitude decreases, as expected. For the samples which were not fractured after 10^7 cycles. The test was stopped and these specimens were indicated as run-out samples by arrows on S-N curve in Figure.

The stress amplitude at which the sample did not fracture after 10^7 cycles is considered as the fatigue limit. Therefore, it can be concluded that the DIT 280 and QBT sample have the same fatigue limit of 402 MPa. Also, it was determined that there was no significant difference between the number of fracture cycles in the finite life region of the S-N curve. ANOVA analysis was used to statistically evaluate the differences in the number of cycles to fracture of both groups. The Anova analysis results are given in Table 4.9. According to the results, we conclude that there is no significant difference between the groups since the calculated value of F is less than the Fvalue value. Based on the Anova analysis, it was concluded that there was no significant difference between the results even though the hardness, strength and toughness values of the samples changed significantly.

Table 4.8 : Fatigue test results of QBT200 and DIT280 samples.

Test No	OBT200		DIT280	
	Stress amplitude (MPa)	Number of cycles	Stress amplitude (MPa)	Number of cycles
1	402	10,155,631*	402	10,139,925*
2	405	5,889,205	460	101,066
3	455	1,238,598	460	289,778
4	460	167,546	494	140,082
5	494	75,656	494	392,446

*the sample did not fracture after 10^7 cycles.

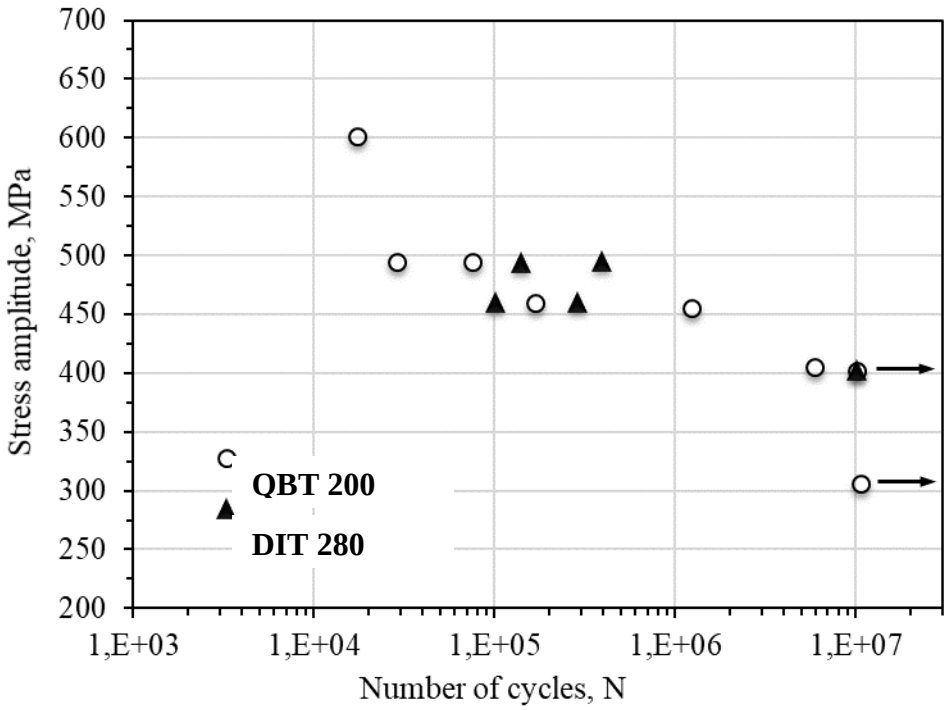

Figure 4.14 : S-N curve of DIT 280 and QBT 200 samples.

Table 4.9 : Anova analysis evaluation of QBT 200 and DIT 280 fatigue test results.

	QBT 200	DIT 280
Mean	3300850.4	2212659.4
Variance	2.29339E+13	1.96516E+13
Value	5	5
df	4	4
Fcalculated	1.167023986	
P(F<=f)	0.442308007	
Fvalue	6.388232909	

4.5 Fractography

4.5.1 Tensile test samples

The fracture surfaces of the tensile specimens were examined by visually and with SEM (Figure 4.15). As a result of macro-scale examinations, shear lips were seen at the edges of the sample. In micro-scale examinations, cleavage facets, dimple formation and secondary cracks were observed in the fracture surfaces.

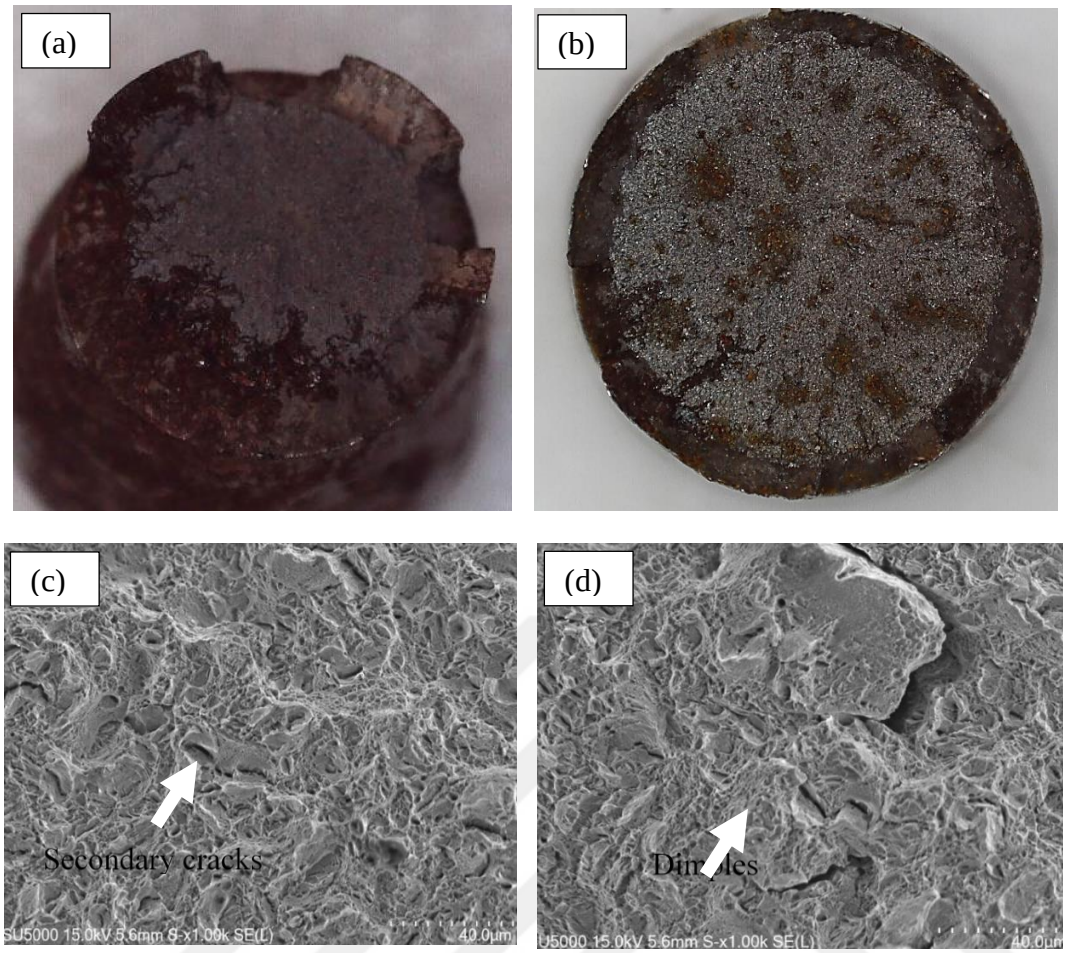

Figure 4.15 : (a-c) Macro and microfracture surfaces of QBT200 sample after the tensile test, (b-d) Macro and microfracture surfaces of DIT280 sample after the tensile test.

4.5.2 Fatigue test samples

The fracture surfaces of the fatigue samples were examined with SEM (Figure 4.16). Crack initiation, crack propagation and final fracture regions were observed. When macroscopic examinations were made, a smooth fracture was detected in both heat treatment conditions.

As it is known, fatigue fracture surfaces of metallic materials are characterized by beach marks. When both heat treatment samples are examined, beach marks are not clearly visible because of the samples tested in constant amplitude. Nevertheless some radial marks are visible (indicated by dashed lines in te fracture surfaces). The crack initiation point is shown with an arrow. The cracks start from a single point on the sample surface, indicating that there is no circumferential notch effect on the samples.

When microscopic examinations are made in the crack propagation area, dimples and cleavage fracture characteristics were observed. Observation of both cleavage fracture

and ductile fracture characteristics such as dimple in the fracture surface shows that the observed fracture was quasi cleavage. Additionally it was observed that as the martensite volume ratio increases, the fractured surfaces become smoother and more brittle. Direct Isothermal heat treated sample (DIT280) have more dimples and voids while in the structure quenched at 200 °C before isothermal transformation (QBT 200) have more cleavege facets. As a result, although brittle fracture was observed on a macroscopic scale, both ductile and brittle fracture characteristics were observed on a microscopic scale.

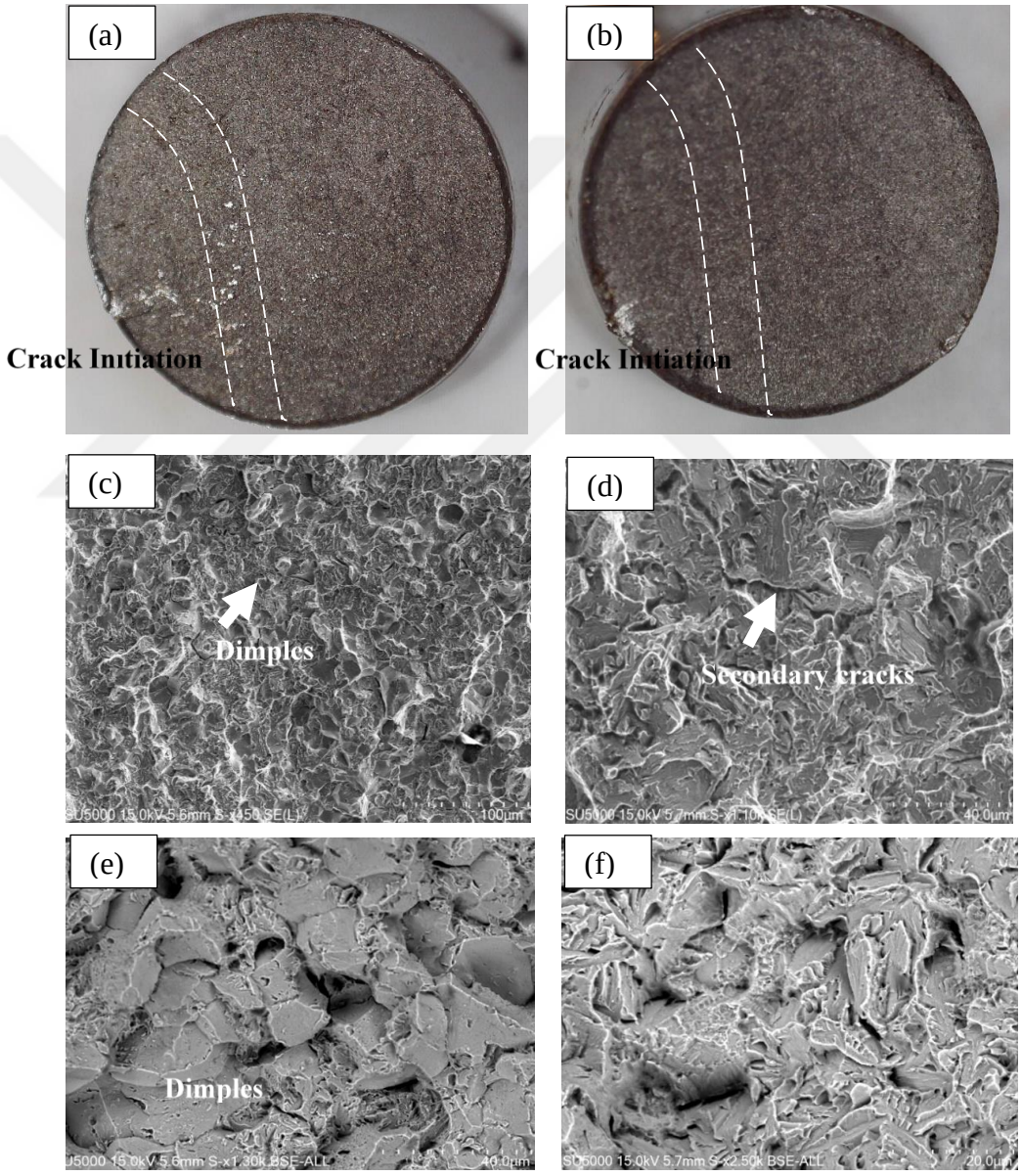

Figure 4.16 : (a-c-e) Macro and microfracture surfaces of QBT200 sample after fatigue test , (b-d-f) Macro and microfracture surfaces of DIT280 sample after fatigue test.

6. CONCLUSIONS

The following conclusisons can be drawn from the present thesis:

- Ms temperature was determined as 250 °C. TTT diagram was constructed with JmatPro software.
- Volume fraction of martensite decreases and bainite volume fraction increases, which are accompanied by a decrease in hardness, with the increase in the quenching temperature.
- Martensite volume fraction increased from 10% to 53% when the quench temperature was reduced from 240 °C to 180 °C.
- Depending on the increase in martensite volume fraction, a corresponding increase in hardness from 577 HV to 615 HV (% 6 increase) was observed.
- When direct austempered sample and quenched and austempered samples are compared, hardness decreased from the 615 HV to 548 HV (% 11 reduction) with direct austempering process.
- Yield strengths of QBT 200 and DIT 280 samples are 1920 MPa and 1825 MPa, respectively. (5% reduction), the tensile strengths are 2052 MPa and 1910 MPa, respectively. (7% reduction)
- The impact resistance of QBT 200 and DIT 280 samples are 10 J and 33 J, respectively. This result shows that the structure consisting entirely of bainite has better toughness than the martensite-bainite duplex structure.
- While brittle fracture was detected on the macro scale, ductile fracture characteristics were also detected on the micro scale.
- Unlike the hardness, tensile and impact test results, no significant difference was observed between the fatigue test results.

REFERENCES

[1] **S. M. Hasan, S. Kumar, D. Chakrabarti, and S. B. Singh**, (2020) "Understanding the effect of prior bainite/martensite on the formation of carbide-free bainite", *Philos. Mag.*, c. 100, sy 7, ss. 797-821.

[2] **M. J. Santofimia,** (2013) "Combining bainite and martensite in steel microstructures for light weight applications", c. 113.

[3] **X. Lu, Z. Yang, D. Qian, J. Lan, ve L. Hua**, (2021) "Effect of martensite pre-quenching on bainite transformation kinetics, martensite/bainite duplex microstructures, mechanical properties and retained austenite stability of GCr15 bearing steel", *J. Mater. Res. Technol.*, 15, 2429-2438.

[4] **Y. Tomita,** (2000**)** "Development of fracture toughness of ultrahigh strength, medium carbon, low alloy steels for aerospace applications", *Int. Mater. Rev.*, c. 45, sy 1, ss. 27-37.

[5] **M. Morawiec, A. Skowronek, A. Kozłowska, C. Garcia-Mateo, and A. Grajcar,** (2023) "Effect of prior martensite formation on the bainite transformation kinetics in high-strength 3% Mn multiphase steel", *J. Therm. Anal. Calorim.*, c. 148, sy 4, ss. 1365-1371.

[6] **H. Guo, X. Feng, A. Zhao, Q. Li, and J. Ma,** (2019) "Influence of Prior Martensite on Bainite Transformation, Microstructures, and Mechanical Properties in Ultra-Fine Bainitic Steel", *Materials*, c. 12, sy 3, s. 527.

[7] **A. Navarro-López, J. Sietsma, and M. J. Santofimia,** (2016)"Effect of Prior Athermal Martensite on the Isothermal Transformation Kinetics Below M s in a Low-C High-Si Steel", *Metall. Mater. Trans. A*, c. 47, sy 3, ss. 1028-1039.

[8] **H. Guo, X. Feng, A. Zhao, Q. Li, and J. Ma,** (2019)"Influence of Prior Martensite on Bainite Transformation, Microstructures, and Mechanical Properties in Ultra-Fine Bainitic Steel", *Materials*, c. 12, sy 3, s. 527.

[9] **A. S. Schulz-Beenken,** (1997)"Martensite in Steels : its Significance, Recent Developments and Trends", *J. Phys. IV*, c. 07, sy C5, ss. C5-359-C5-366.

[10] **T. Maki,** "Morphology and substructure of martensite in steels", içinde *Phase Transformations in Steels*, Elsevier, 2012, ss. 34-58.

[11] **R. J. Wasilewski,** (1975) "On the nature of the martensitic transformation", *Metall. Trans. A*, c. 6, sy 7, ss. 1405-1418.

[12] **P. M. Kelly and J. Nutting**, (1960) "The martensite transformation in carbon steels", *Proc. R. Soc. Lond. Ser. Math. Phys. Sci.*, c. 259, sy 1296, ss. 45-58, Kas. 1960.

[13] **A. S. Schulz-Beenken,** (1997)"Martensite in Steels : its Significance, Recent Developments and Trends", *J. Phys. IV*, c. 07, sy C5, ss. C5-359-C5-366.

[14] **A. Saastamoinen,** "Processing and microstructure of direct-quenched and tempered ultra-high strength steels".

[15] **M. Azuma, N. Fujita, M. Takahashi, T. Senuma, D. Quidort, ve T. Lung, (**2005)"Modelling Upper and Lower Bainite Trasformation in Steels", *ISIJ Int.*, c. 45, sy 2, ss. 221-228.

[16] **L. Qian, Z. Li, T. Wang, D. Li, F. Zhang, ve J. Meng,** (2022)"Roles of pre-formed martensite in below-Ms bainite formation, microstructure, strain partitioning and impact absorption energies of low-carbon bainitic steel", *J. Mater. Sci. Technol.*, c. 96, ss. 69-84, Oca.

[17] **M. Takahashi,** (2004)"Recent progress: kinetics of the bainite transformation in steels", *Curr. Opin. Solid State Mater. Sci.*, c. 8, sy 3-4, ss. 213-217.

[18] **K. Chen, H. Lia, Z. Jiang, F. Liu, C. Kang, X. Ma, B. Zhao,** (2021)"Multiphase microstructure formation and its effect on fracture behavior of medium carbon high silicon high strength steel", *J. Mater. Sci. Technol.*, c. 72, ss. 81-92.

[19] **M. S. Htun, S. T. Kyaw, and K. T. Lwin,** (2008)"Effect of Heat Treatment on Microstructures and Mechanical Properties of Spring Steel".

[20] **M.-S. Suh, S.-H. Nahm, C.-M. Suh, and N.-K. Park,** (2022)"Impact Toughness of Spring Steel after Bainite and Martensite Transformation", *Metals*, c. 12, sy 2, s. 304,

[21] **Y. Toji, H. Matsuda, and D. Raabe,** (2016)"Effect of Si on the acceleration of bainite transformation by pre-existing martensite", *Acta Mater.*, c. 116, ss. 250-262,

[22] **L. Zhang, D. Gong, Y. Li, X. Wang, X. Ren, and E. Wang, (**2018)"Effect of Quenching Conditions on the Microstructure and Mechanical Properties of 51CrV4 Spring Steel", *Metals*, c. 8, sy 12, s. 1056.

[23] **E. Claesson,** (2014) "Development of a heat treatment method to form a duplex microstructure of lower bainite and martensite in AISI 4140 steel".

CURRICULUM VITAE

Name Surname **:** Şeyma UĞUR

EDUCATION **:**

- **B.Sc.** **:** 2020, Istanbul University, Engineering Faculty, DeparMetallurgical and Materials Engineering

PROFESSIONAL EXPERIENCE AND REWARDS:

- 2022- Materials and Special Process Engineer at BAYKAR
- 2021-2022 Project Engineer at Şahin Metal
- 2019- Internship at TÜBİTAK MAM

PUBLICATIONS, PRESENTATIONS AND PATENTS ON THE THESIS:

- **Uğur Ş.,** Elmalı Ü., Balcı E., Baydoğan M., "The Effect of Successive Quenching and Austempering Heat Treatments on the Microstructure of a High Silicon Steel" International Graduate Research Symposium (IGRS'24), İstanbul, Türkiye, 8-10 Mayıs, 2024.